

## ARTICLE

<https://doi.org/10.1038/s42004-019-0153-0>

OPEN

# The role of adsorbates in the green emission and conductivity of zinc oxide

Jason A. Röhr<sup>1,2</sup>, Jacinto Sá<sup>3,4</sup>  & Steven J. Konezny<sup>1,2</sup> 

Zinc oxide is a versatile semiconductor with an expansive range of applications including lighting, sensing and solar energy conversion. Two central phenomena coupled to its performance that remain heavily investigated are the origin of its sub-band-gap green emission and the nature of its conductivity. We report photoluminescence and dark conductivity measurements of zinc oxide nanoparticle films under various atmospheric conditions that demonstrate the vital role of adsorbates. We show that the UV emission and conductivity can be tuned reversibly by facilitating the adsorption of species that either donate or extract electrons from the conduction band. When the conductivity data are compared with photoluminescence spectra taken under the same ambient conditions, the green emission can be directly linked to surface superoxide formation, rather than surface hydroxylation or native defects such as oxygen vacancies. This demonstrates how and explains why the green emission can be controlled by surface reactivity and chemical environment.

<sup>1</sup>Energy Sciences Institute, Yale University, 520 West Campus Drive, West Haven, CT 06516, USA. <sup>2</sup>Department of Chemistry, Yale University, 225 Prospect Street, New Haven, CT 06511, USA. <sup>3</sup>Department of Chemistry, Ångström Laboratory, Uppsala University, 75120 Uppsala, Sweden. <sup>4</sup>Institute of Physical Chemistry, Polish Academy of Sciences, 01-224 Warsaw, Poland. Correspondence and requests for materials should be addressed to S.J.K. (email: [steven.konezny@yale.edu](mailto:steven.konezny@yale.edu))

Zinc oxide (ZnO) nanoparticles and nanowires have gained considerable attention due to a wide variety of potential applications including gas sensors<sup>1,2</sup>, solar cells<sup>3,4</sup>, UV light-emitting diodes<sup>5</sup> and lasers<sup>6</sup>, and solar-driven water-splitting cells<sup>7</sup>. Mesoporous ZnO is a particularly attractive alternative to incumbent technologies because of benefits such as low cost, material abundance, large surface area, low toxicity and relatively large charge-carrier mobilities<sup>8,9</sup>. Nanoparticle ZnO thin films have a large surface-area-to-volume ratio and therefore contain a high density and wide variety of unavoidable surface defects<sup>10</sup>. They can also adsorb a large amount and variety of gas molecules<sup>1,2</sup>. Some of these defects and interactions are a technological advantage, while others are reportedly responsible for unwanted sub-band-gap green emission and extrinsic conductivity in ZnO. For ZnO films to be useful in commercially viable technologies, the origin of these defects must be understood in order to suppress the green emission, tune the electrical properties to either n-type or p-type and control the surface defects to match the redox potentials for catalytically driven reactions.

Native defects on metal oxide nanostructures, such as vacancies, interstitials and antisites, are inevitable<sup>10</sup>, and these defects are in part responsible for giving many metal oxides important electrical and catalytic properties<sup>11</sup>. Because oxygen vacancies, compensated by free electrons, give rise to n-type conductivity in TiO<sub>2</sub><sup>12,13</sup>, this was also thought to be the case for ZnO. Early theoretical studies and measurements of higher conductivities under oxygen-poor conditions suggested that oxygen vacancies and zinc interstitials were likely candidates for causing n-type conductivity in ZnO<sup>13,14</sup>. However, later calculations identified oxygen vacancies as very deep donors, and therefore not thermally active at room temperature<sup>15,16</sup>. These same studies showed that zinc interstitials are highly unstable and are therefore not expected to be present in appreciable quantities. In fact, calculated formation energies and energy levels of potential native point defects in ZnO nanostructures suggest they are either unstable or too deep to be electron donors and are therefore unlikely to be the cause of the n-type conductivity<sup>17</sup>.

Native defects have also been considered as the source of the observed sub-band gap green emission in ZnO<sup>17</sup>. The photoluminescence (PL) of ZnO nanoparticles has two emission peaks: a sharp UV peak due to emission from band-to-band recombination and a broad green emission peak arising from trap-assisted recombination<sup>18–20</sup>. In spite of extensive investigations into the emissive properties of ZnO, it is still not entirely understood whether native defects are the cause of the unwanted green emission, and if they are, which defects are responsible<sup>16,17</sup>. Most experimental and theoretical studies have attributed the green emission to recombination of free holes with trapped electrons in oxygen vacancies<sup>21–23</sup>, in zinc interstitials and antisites<sup>24</sup>, or free electrons with holes trapped in zinc vacancies<sup>22,23</sup>, oxygen interstitials and/or antisites<sup>16</sup>, without reaching a consensus.

Adsorbed species on the nanoparticle surface play a central role in charge transport<sup>25,26</sup>. This interaction has been studied extensively and is the basis of the gas sensing capabilities of ZnO<sup>1,2</sup>. Changes in the relative concentrations of potential adsorbates in the atmosphere lead to detectable changes in the conductivity. Particular adsorbates can increase or decrease the conductivity depending on their electron donating or withdrawing character, respectively, since this will have an impact on the charge carrier density in n-type ZnO. In addition to adsorbates that originate from material synthesis and preparation, such as hydrogen binding to unterminated oxygen<sup>27</sup>, a host of chemical species are present in air which can readily adsorb to ZnO, such as O<sub>2</sub>, H<sub>2</sub>O and CO<sub>2</sub><sup>28</sup>. For example, nanostructured ZnO can be used as an oxygen sensor because molecular oxygen can

bind to ZnO by capturing an electron from the conduction band to form chemisorbed superoxide O<sub>2</sub><sup>-</sup>, which results in a measurable decrease in conductivity<sup>2,29</sup>. The opposite effect can be seen in the adsorption of water, which can dissociate into surface hydrogen and hydroxyl groups<sup>11,30</sup>. Hydrogen, both as an interstitial and bound to an oxygen vacancy, has been suggested to be the primary source of electron donor sites in ZnO, and hence the main cause for its n-type conductivity<sup>25,26</sup>.

There is evidence suggesting that adsorbed species, rather than native defects, are the main contributors to the green emission<sup>31</sup>. For instance, hydroxylation of oxygen vacancies was suggested to be the source of green emission, which is consistent with the observation that the sub-band-gap emission was suppressed when measured under vacuum<sup>32</sup>. However, to the authors knowledge, the role of adsorbates on the emissive properties of ZnO is relatively unexplored, with only one other publication showing that the green emission from ZnO nanoparticles is highly affected by the molecular content of the ambient<sup>33</sup>.

In this work, we take advantage of the gas sensing capabilities of ZnO and combine PL and electrical conductivity measurements, under various atmospheric conditions, as a systematic way of determining the role of adsorbates in the green emission and conductivity of nanostructured ZnO. Our approach enables the monitoring of PL shifts caused by changes in the relative concentrations of adsorbed species as a function of time, both during gas exposure and upon UV photodesorption. The PL is dominated by green emission under oxygen-rich conditions, which points to adsorbed oxygen as the source of green emission. Furthermore, since a significant decrease in the conductivity under these same oxygen-rich conditions is observed, and since the green emission is caused by trap-assisted recombination, we propose that the origin of green emission in ZnO is due to adsorbed O<sub>2</sub><sup>-</sup>, which, to the authors knowledge has never been considered.

## Results

### Photoluminescent response in different ambient conditions.

The relative intensities of green (~2.3 eV) and UV emission (~3.3 eV) have been used to characterize emissive defects in ZnO<sup>19,31</sup>. This has typically been done to compare samples annealed at different temperatures or conditions, e.g., in zinc- or oxygen-rich environments, to manipulate the concentrations of specific native defects<sup>22–24</sup>. However, the ambient atmosphere, and the resulting adsorbed species on the surface, is often ignored during PL measurements, even though its chemical composition governs the conductivity of ZnO<sup>2,25,29,31</sup>. We used steady-state PL measurements in various atmospheres, recorded over several hours, to monitor changes in the spectra caused by adsorption and UV-induced desorption of chemical species.

Figure 1 shows PL emission of a ZnO nanoparticle thin film excited with 4.13 eV light (300 nm), that is, light with an energy exceeding the ZnO band gap of approximately 3.25 eV (see Supplementary Fig. 1). Each curve corresponds to a measurement with duration of approximately 1 min and 50 seconds performed at room temperature. Figure 1a shows the emission in air, i.e., an atmosphere consisting of mixed gases of mostly N<sub>2</sub>, O<sub>2</sub> and H<sub>2</sub>O, when illuminated over the course of ~4 h. The green emission intensity was initially low as compared to the UV emission. Over the course of the experiment in air, the UV emission decreases and the green emission peak rises with an apparent slight shift to lower energy. Figure 1b shows emission from the sample as the atmosphere is quickly changed from air to vacuum and then monitored over 2 h. This led to a rapid decrease in the green emission intensity. Figure 1c shows emission from the sample under vacuum for a duration of ~6 h,

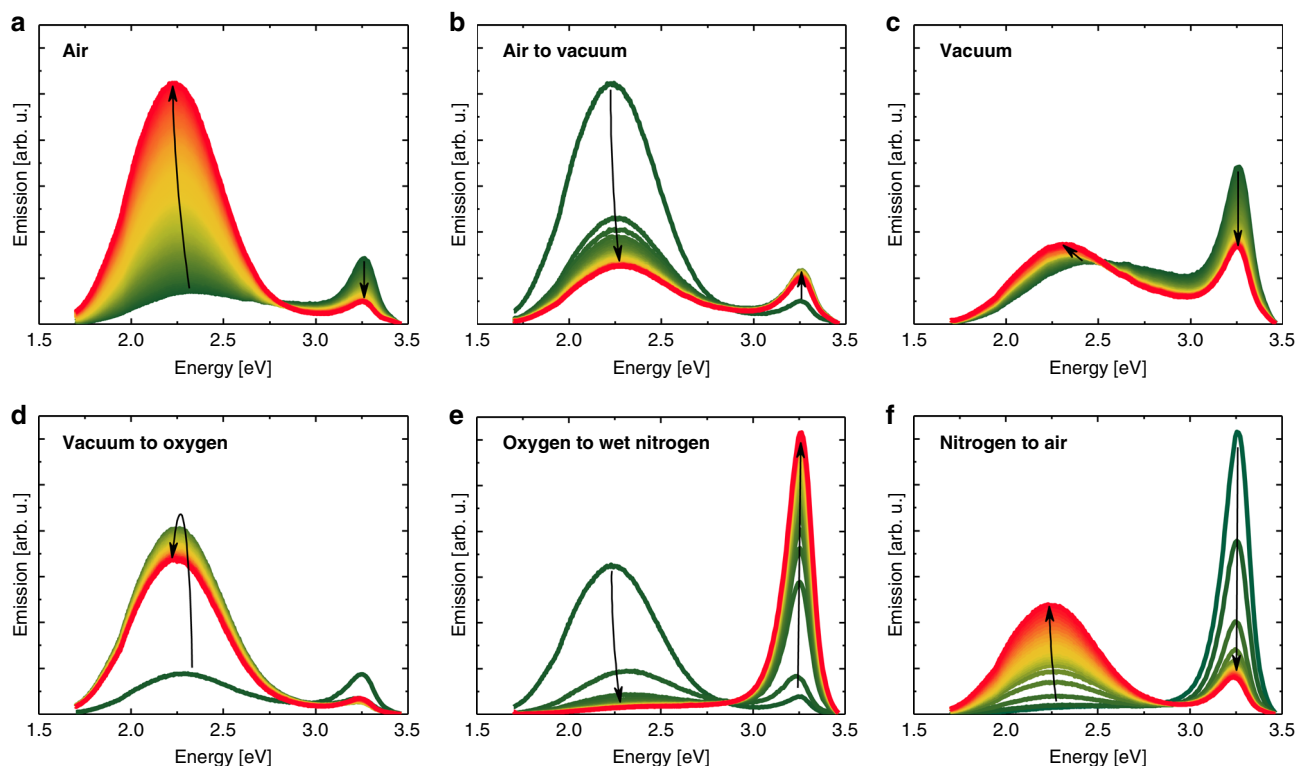


**Fig. 1** PL emission measured from 1.7eV to 3.45eV under different atmospheric conditions: **a** air, **b** air to vacuum, **c** measured entirely under vacuum, **d** measured as oxygen was introduced after being kept in vacuum, **e** oxygen displaced by nitrogen containing water vapour and **f** dry nitrogen to air. Arrows and changes in colour from green to red show passing of time

where a similar apparent shift is observed as the green emission peak grows.

Figure 1d shows emission as the atmosphere is changed from vacuum to pure oxygen for 1 h and 23 minutes. This change led to an initial rapid increase in the green emission due to the sudden injection of oxygen into the system. This rapid increase is in contrast to what was observed in the mixed-gas system presented in Fig. 1a, indicating that adsorbed oxygen is responsible for green emission and that more than one species of adsorbate is occupying adsorption sites in the mixed gas system. Figure 1e shows the emission over a duration of 1 h and 22 minutes following a replacement of the oxygen atmosphere with nitrogen and water vapour. This led to a quick drop, and an eventual quench, of the green emission and an abrupt increase in the UV emission. When dry nitrogen is replaced with air as shown in Fig. 1f (experiment duration: 29 minutes), the behaviour in air, as seen in Fig. 1a, is recovered. No appreciable changes were observed between the emission measured in wet and dry nitrogen, indicating that neither nitrogen nor water had an observed effect on the emissive properties (see Supplementary Fig. 2).

Figure 2 shows the results of fitting the PL spectra with gaussian peaks including two example spectra taken in air before (Fig. 2a) and ~4 h into (Fig. 2b) the growth of the green emission upon UV illumination. The green emission does not shift, but rather, it comprises two peaks centred at 2.24 eV and 2.65 eV. The increase in green emission is dominated by the growth in the 2.24 eV peak. This can be clearly seen in Fig. 2c, d, which show the integrated peak emission as a function of time as the ambient conditions are abruptly changed between oxygen-rich and oxygen-poor conditions. The 2.24 eV peak is highly sensitive to the presence of oxygen.

**Transient conductivity measurements.** Conductivity measurements provide sensitivity to adsorbates, which has been

repeatedly demonstrated in ZnO in the context of sensors. Since ZnO is highly sensitive to adsorbates<sup>2,25,29</sup>, transient conductivity measurements can be used as a tool to investigate how the charge-carrier densities are affected by oxygen, water and nitrogen. Figure 3a shows the current and atmospheric pressure as a function of time when the ambient atmosphere is evacuated. The conductivity gradually increases as the pressure slowly decreases. Figure 3b shows the current and pressure as pure oxygen is introduced, giving rise to a slow and gradual decrease in the conductivity. Figure 3c shows the conductivity and relative humidity under vacuum after equilibrating under vacuum. When an atmosphere consisting of nitrogen and water vapour is abruptly introduced, the conductivity increases significantly and the current response proportional to the relative humidity. Figure 3d shows the current and pressure as dry nitrogen was introduced, showing no significant change.

#### Adsorption-induced changes in emission and conductivity.

Several important observations can be made when monitoring the PL over an extended period following an abrupt change in ambient atmospheric conditions, as shown in Fig. 1. The relative intensities of the emission peaks can be strongly dependent on both the atmosphere and the duration of successive PL measurements. The rate of change of the emission spectra provides additional information. The fact that these changes can occur over several hours is consistent with adsorption processes, particularly in the case of mixed gases when there is a competition between adsorption (see Fig. 2a), photo-induced desorption, and adsorbate displacement. ZnO is known to adsorb many gases including O<sub>2</sub>, H<sub>2</sub>O and CO<sub>2</sub><sup>28,34</sup>. By pairing PL and conductivity measurements one can begin to make systematic observations regarding which adsorbates do, and do not, impact the green emission. In this section we show the role of adsorbates on the

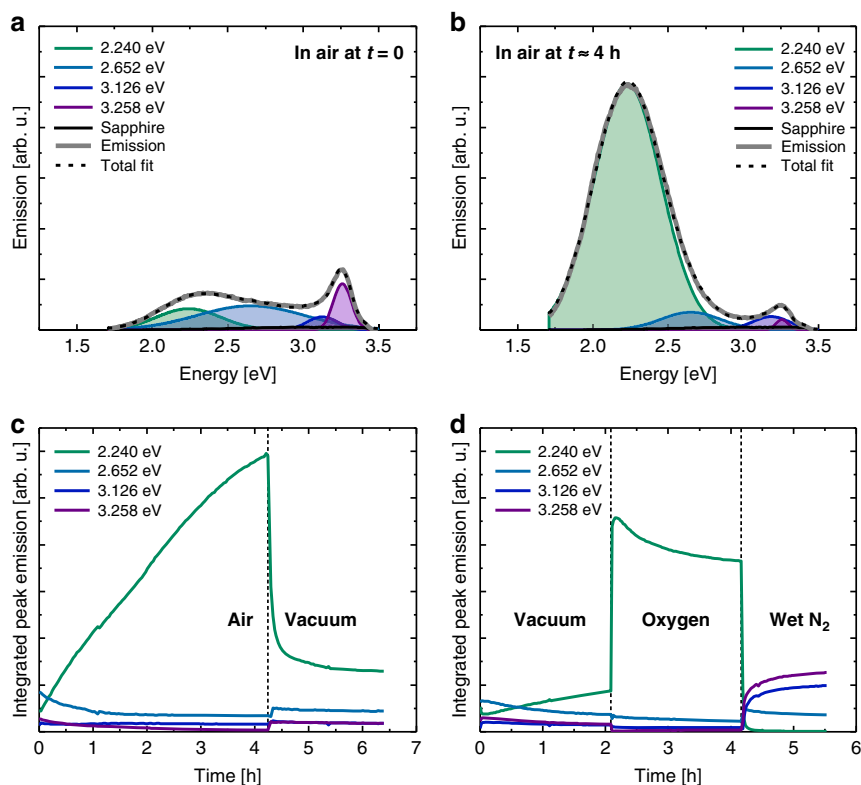


**Fig. 2** Gaussian fits and time evolution of emission peaks: PL emission profiles between fitted with Gaussian functions and the reflectance profile of the sapphire substrate. **a** Emission profile when initially measured in air. **b** Emission after the sample was measured continuously in air for  $\sim 4$  h. **c** Integrated peak emission, obtained from fitting with Gaussian peaks, when the sample was measured in air and vacuum. **d** Integrated peak emission when the sample was measured in vacuum and oxygen

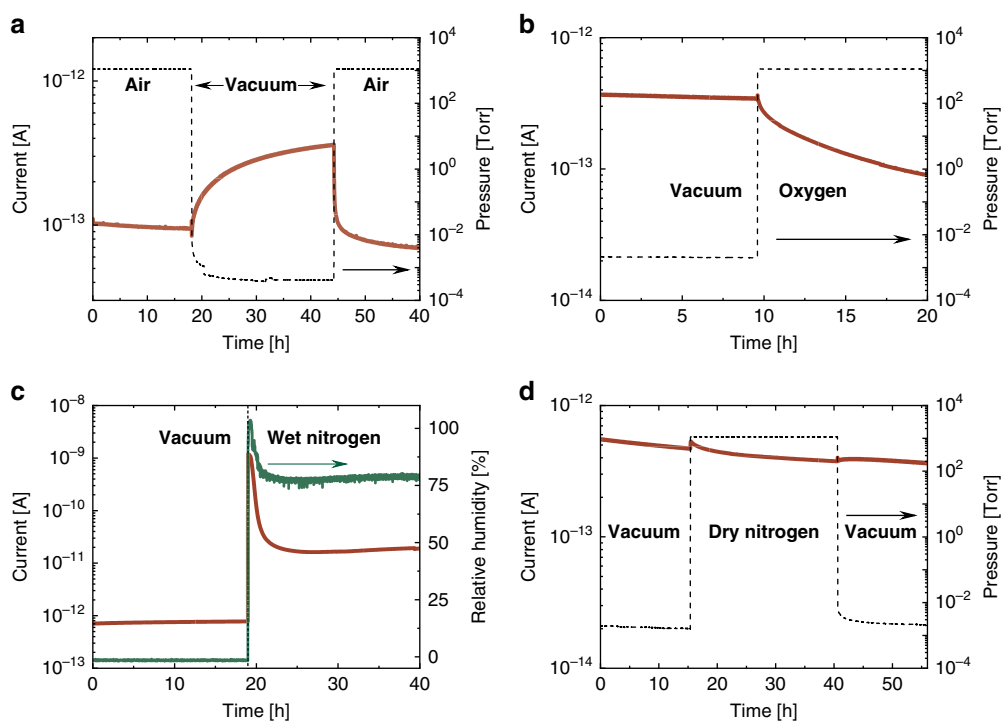


**Fig. 3** Conductivity measurements in different atmospheres: **a** Current, measured at 2 V, and pressure as a function of time when the atmosphere is evacuated for 18 h and subsequently vented with air. **b** Current and pressure as pure oxygen is introduced. **c** Current and relative humidity under vacuum and in a nitrogen atmosphere containing water vapour. **d** Current and pressure as dry nitrogen is introduced for approximately 25.5 h. The relative humidity is negligible in dry nitrogen, pure oxygen and vacuum cases

fluorescence and conductivity of ZnO in the presence of water, oxygen and then air, which is a more complicated mixed gas system.

The ability of ZnO to adsorb water, and the effect this has on the conductivity, is demonstrated in Fig. 3b. Initially, the sample is under vacuum, a situation in which the surface is expected to have a more reactive surface with many available adsorption sites. The introduction of water vapour increased the conductivity of the ZnO nanoparticle film by orders of magnitude. The fact that the introduction of dry N<sub>2</sub> gas in Fig. 3d did not have an effect on the conductivity means that the effects of wet N<sub>2</sub> gas are due to the water vapour alone. This is consistent with the humidity sensing abilities of ZnO<sup>35</sup> and previous studies suggesting that dissociated water, leading to bound hydrogen, is the primary cause of the extrinsic conductivity<sup>25,36,37</sup>. This process of dissociating water on the ZnO surface, however, had no impact on the shape or intensity of the emission profile as seen in Supplementary Fig. 2. This rules out hydroxylation as the cause of green emission.

The green emission quickly dominates the emission profile as pure oxygen is introduced to the sample (see Fig. 1d), whereas the green emission is entirely quenched, with UV dominating the PL signal, when nitrogen (either wet or dry) is introduced. This is in agreement with previous published results, where it was shown that the change in intensity of the green emission in ZnO increases with smaller particle sizes<sup>33</sup>. If oxygen vacancies were the cause of green emission, this emission should not decrease when switching from oxygen-rich to inert, oxygen-poor environments. However, the green emission is highly pronounced in oxygen, and completely quenched in nitrogen (see Fig. 4a). When coupled with the conductivity results, this strongly suggests that oxygen adsorbing to the ZnO surface, rather than oxygen vacancy formation, leads to green emission in ZnO nanoparticles.

Molecular oxygen is known to be an excellent electron scavenger when adsorbing onto electron rich materials, readily forming negatively charged superoxide O<sub>2</sub><sup>-</sup><sup>2,29</sup>. The conductivity significantly increases when the mixed gas atmosphere surrounding the sample is evacuated (see Fig. 3a) and the conductivity largely decreases when pure oxygen is injected into the chamber (see Fig. 3b). These observations are consistent with O<sub>2</sub><sup>-</sup> formation on the ZnO particle surface caused by oxygen adsorption and an accompanying electron transfer. An estimate of the number of adsorption events is given in Supplementary Note 1 and Supplementary Fig. 3. These electrons are injected back into the ZnO conduction band when the oxygen molecules desorb from the surface. Since O<sub>2</sub> effectively acts as an electron trap when forming O<sub>2</sub><sup>-</sup>, and since the green emission is caused by the presence of O<sub>2</sub>, the most likely recombination process leading

to green emission is between a trapped electron at the O<sub>2</sub><sup>-</sup> site and a free hole in the valence band (Fig. 4b). Since we observe that the green emission, observed in the oxygen-rich environment, is comprised of a single peak at 2.24 eV (see Fig. 2c, d), we place the O<sub>2</sub><sup>-</sup> defect level at the same energy above the ZnO valence band edge. Dynamic and reversible fluorescence triggered by superoxide has been extensively reported in live-cell imaging, but to our knowledge has never been linked to solid-state material photoluminescence<sup>38</sup>.

We are able to see the evolution of the 2.24 eV peak and changes in the conductivity so clearly because of the high surface area of our ZnO films cast from 10 nm particles. Studies of ZnO particles of varying in size from 5 to 15 nm show that the green emission of smaller particles is more susceptible to changes in the atmosphere<sup>33</sup>. It is possible that other defect levels, like the one at 2.65 eV, become more relevant in ZnO when its surface-to-volume ratio is much smaller, as in epitaxially grown films. However, in the case of nanostructured ZnO films, adsorbed superoxide is most important and the emission can be tuned from green to UV by controlling the oxygen content of the atmosphere as shown in Fig. 4.

The case of mixed gases is more complicated, but particularly relevant as most reports of photoluminescence are taken in air. By comparing the spectra in Fig. 1a, d it can be seen that the presence of chemical species besides oxygen in the atmosphere, such as H<sub>2</sub>O and CO<sub>2</sub>, causes a gradual increase in the green emission rather than the abrupt transitions observed when pure oxygen is introduced. As both dry and wet nitrogen led to quenching of the green emission, the slow increase observed in Fig. 1a is most likely due to a competition between adsorption of all the species present in the atmosphere. With all species gradually desorbing as the sample is illuminated with UV light, a larger density of O<sub>2</sub> molecules are allowed to adsorb as it is more prevalent in air. The growth of the green emission peak occurred over many hours in ambient atmosphere (see Fig. 1a) and the quenching of the green emission when an overpressure of nitrogen was introduced (see Fig. 1e) indicate that the ZnO surface has a propensity towards the adsorption of molecules other than O<sub>2</sub>. It also indicates that an additional driving force, such as UV exposure by the excitation source of the PL measurement, is required to observe significant green emission in air.

## Discussion

We have shown that both the emission and the conductivity of ZnO are highly sensitive to the composition of the ambient atmosphere. The green part of the emission increases drastically under oxygen-rich conditions, which is accompanied by a decrease in both the conductivity and the UV emission. This shows that the green

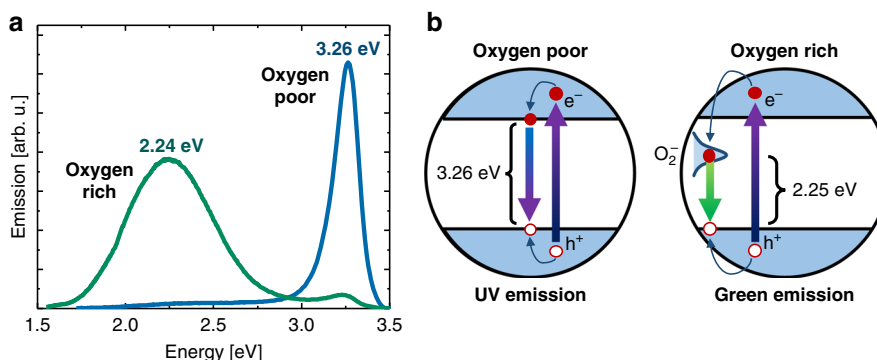


**Fig. 4** Oxygen adsorption process and green emission mechanism: **a** Emission profiles of ZnO thin films in oxygen and nitrogen atmospheres with peaks centred at 2.24 eV (green) and 3.26 eV (UV), respectively. **b** Schematic showing the recombination between free charge carriers leading to UV emission. **c** Recombination between a trapped electron on a superoxide and a free hole leading to green emission in the oxygen rich environment

emission is not caused by oxygen vacancies, but rather by trap-assisted recombination via superoxide species on the particle surface with a defect level located at 2.24 eV above the valence band edge. Where water vapour was found to drastically increase the conductivity, it had no effect on the emission. We demonstrate that UV exposure, even by the excitation source in a PL measurement, can shift the population of adsorbed species on the ZnO surface and modify the relative intensity of emissive peaks, and must be taken into account in interpreting PL results. Our results show that the emission and conductivity of ZnO can be readily tuned by simply controlling the oxygen content and water vapour in the atmosphere surrounding the sample. The material emission is directly affected by surface reactivity and chemical atmosphere.

## Methods

**ZnO nanoparticles and sample preparation.** Water-soluble ZnO particles (~10 nm in diameter) functionalized with carboxylate oligoethylene glycol were used in this study for improved film processing. Details of the particle synthesis including electron microscopy characterisation is reported in a previous publication<sup>39</sup>. All films used for UV-vis absorbance, PL and conductivity measurements were fabricated by spin casting a 205 mg/mL ZnO water solution onto cleaned sapphire (Al<sub>2</sub>O<sub>3</sub>) substrates.

**UV-Vis and PL.** Absorbance curves of the ZnO films were obtained from transmittance and reflectance measurements using a Shimadzu UV-2600 spectrometer with an integrating sphere. All PL spectra were acquired using a Horiba Scientific FluoroMax Spectrofluorometer with a 300 nm excitation source at a duration of 1 min and 53 seconds at 10 second intervals. A 355-nm long-wave pass filter was used to limit optical artefacts. Oxygen was introduced directly from a gas cylinder whereas gaseous nitrogen was fed through an oxygen/moisture trap filter that reduces oxygen to <2 ppb. Water vapour was introduced by bubbling nitrogen in deionized water in a closed system. For PL measurements under vacuum, a roughing pump that achieves a maximum vacuum of 6.8 Torr was used.

**Conductivity measurements.** Interdigitated top electrodes for conductivity measurements were deposited by thermal evaporation of Cr/Au through a shadow mask. We use coplanar contacts so that exposure of the active area to the atmosphere is the same as in the PL measurements. Highly sensitive electrical measurements were performed inside a cryostat with significant electrical shielding using an Agilent B1500A semiconductor device analyser equipped with source-measurement modules and atto-sense units. Gasses were introduced in a similar way to how they were introduced during the PL measurements. Lower pressures reported for conductivity measurements under vacuum were achieved using a turbo pump. The accuracy of the humidity sensor mounted in the cryostat was ±3.5% relative humidity. The current was measured at an applied voltage of 2 V for all electrical measurements.

## Data availability

All data supporting the findings of this study are available in the paper and the Supplementary Information file, as well as available from the corresponding author upon reasonable request.

Received: 9 January 2019 Accepted: 8 April 2019

Published online: 02 May 2019

## References

- Jiang, C., Markutsya, S., Pikus, Y. & Tsukruk, V. V. Freely suspended nanocomposite membranes as highly sensitive sensors. *Nat. Mater.* **3**, 721–728 (2004).
- Sadek, A. Z., Choopun, S., Wlodarski, W., Ippolito, S. J. & Kalantar-zadeh, K. Characterization of ZnO nanobelt-based gas sensor for H<sub>2</sub>, NO<sub>2</sub>, and hydrocarbon sensing. *IEEE Sens. J.* **7**, 919–924 (2007).
- Keis, K., Magnusson, E., Lindstrom, H., Lindquist, S.-E. & Hagfeldt, A. A 5% efficient photoelectrochemical solar cell based on nanostructured ZnO electrodes. *Sol. Energy Mater. Sol. Cells* **73**, 51–58 (2002).
- Zhang, Q., Dandeneau, C. S., Zhou, X. & Cao, G. ZnO nanostructures for dye-sensitized solar cells. *Adv. Mater.* **21**, 4087–4108 (2009).
- Tsukazaki, A. et al. Repeated temperature modulation epitaxy for p-type doping and light-emitting diode based on ZnO. *Nat. Mater.* **4**, 42–46 (2005).
- Chu, S. et al. Electrically pumped waveguide lasing from ZnO nanowires. *Nat. Nanotechnol.* **6**, 506–510 (2011).
- Maeda, K. et al. GaN:ZnO solid solution as a photocatalyst for visible-light-driven overall water splitting. *J. Am. Chem. Soc.* **127**, 8286–8287 (2005).
- Chandiran, A. K., Abdi-Jalebi, M., Nazeeruddin, M. K. & Grätzel, M. Analysis of electron transfer properties of ZnO and TiO<sub>2</sub> photoanodes for dye-sensitized solar cells. *ACS Nano* **8**, 2261–2268 (2014).
- Özgül, Ü. et al. A comprehensive review of ZnO materials and devices. *J. Appl. Phys.* **98**, 041301(1–103) (2005).
- Kofstad, P. Defects and transport properties of metal oxides. *Oxid. Met.* **44**, 3–27 (1995).
- Henrich, V. E. Metal-oxide surfaces. *Prog. Surf. Sci.* **50**, 77–90 (1995).
- Nowotny, M. K., Bak, T. & Nowotny, J. Electrical properties and defect chemistry of TiO<sub>2</sub> single crystal. I. Electrical. *J. Phys. Chem. B* **110**, 16270–16282 (2006).
- Janotti, A. et al. Hybrid functional studies of the oxygen vacancy in TiO<sub>2</sub>. *Phys. Rev. B* **81**, 085212(1–7) (2010).
- Look, D. C., Hemsley, J. W. & Sizelove, J. R. Residual native shallow donor in ZnO. *Phys. Rev. Lett.* **82**, 2552–2555 (1999).
- Janotti, A. & Van De Walle, C. G. Oxygen vacancies in ZnO. *Appl. Phys. Lett.* **87**, 122102(1–3) (2005).
- Vidya, R. et al. Energetics of intrinsic defects and their complexes in ZnO investigated by density functional calculations. *Phys. Rev. B* **83**, 045206(1–12) (2011).
- Janotti, A. & Van De Walle, C. G. Native point defects in ZnO. *Phys. Rev. B* **76**, 165202(1–22) (2007).
- Jacobsson, T. J. & Edvinsson, T. Absorption and fluorescence spectroscopy of growing ZnO quantum dots: size and band gap correlation and evidence of mobile trap states. *Inorg. Chem.* **50**, 9578–9586 (2011).
- Jacobsson, T. J. & Edvinsson, T. A spectroelectrochemical method for locating fluorescence trap states in nanoparticles and quantum dots. *J. Phys. Chem. C* **117**, 5497–5504 (2013).
- Jacobsson, T. J., Viarbitskaya, S., Mukhtar, E. & Edvinsson, T. A size dependent discontinuous decay rate for the exciton emission in ZnO quantum dots. *Phys. Chem. Chem. Phys.* **16**, 13849–13857 (2014).
- De Angelis, F. & Armelao, L. Optical properties of ZnO nanostructures: a hybrid DFT/TDDFT investigation. *Phys. Chem. Chem. Phys.* **13**, 467–475 (2011).
- Børseth, T. M. et al. Identification of oxygen and zinc vacancy optical signals in ZnO. *Appl. Phys. Lett.* **89**, 262112(1–3) (2006).
- Klason, P. et al. Temperature dependence and decay times of zinc and oxygen vacancy related photoluminescence bands in zinc oxide. *Solid State Commun.* **145**, 321–326 (2008).
- Choi, S. et al. Photophysics of point defects in ZnO nanoparticles. *Adv. Opt. Mater.* **3**, 821–827 (2015).
- Van De Walle, C. G. Hydrogen as a cause of doping in zinc oxide. *Phys. Rev. Lett.* **85**, 1012–1015 (2000).
- Oba, F., Togo, A., Tanaka, I., Paier, J. & Kresse, G. Defect energetics in ZnO: a hybrid hartree-fock density functional study. *Phys. Rev. B* **77**, 245202(1–6) (2008).
- Meyer, B. First-principles study of the polar O-terminated ZnO surface in thermodynamic equilibrium with oxygen and hydrogen. *Phys. Rev. B* **69**, 045416(1–10) (2004).
- Gouvea, D., Ushakov, S. V. & Navrotsky, A. Energetics of CO<sub>2</sub> and H<sub>2</sub>O adsorption on zinc oxide. *Langmuir* **30**, 9091–9097 (2014).
- Wilken, S., Parisi, J. & Borchert, H. Role of oxygen adsorption in nanocrystalline ZnO interfacial layers for polymer-fullerene bulk heterojunction solar cells. *J. Phys. Chem. C* **118**, 19672–19682 (2014).
- Janotti, A. & Van De Walle, C. G. Hydrogen multicentre bonds. *Nat. Mater.* **6**, 44–47 (2007).
- Zhou, H. et al. Behind the weak excitonic emission of ZnO quantum dots: ZnO/Zn(OH)<sub>2</sub> core-shell structure. *Appl. Phys. Lett.* **80**, 210–212 (2002).
- Sharma, A., Singh, B. P., Dhar, S., Gondorf, A. & Spasova, M. Effect of surface groups on the luminescence property of ZnO nanoparticles synthesized by sol-gel route. *Surf. Sci.* **606**, L13–L17 (2012).
- Ghosh, M. et al. Role of ambient air on photoluminescence and electrical conductivity of assembly of ZnO nanoparticles. *J. Appl. Phys.* **110**, 054309 (2011).
- Li, Q. H., Gao, T., Wang, Y. G. & Wang, T. H. Adsorption and desorption of oxygen probed from ZnO nanowire films by photocurrent measurements. *Appl. Phys. Lett.* **86**, 1–3 (2005).
- Zhang, Y. et al. Zinc oxide nanorod and nanowire for humidity sensor. *Appl. Surf. Sci.* **242**, 212–217 (2005).
- Ghosh, M., Gadkari, S. C. & Gupta, S. K. Redox reaction based negative differential resistance and bistability in nanoparticulate ZnO films. *J. Appl. Phys.* **112**, 024314 (2012).
- Ramgir, N. S. et al. Growth and gas sensing characteristics of P- and N-type ZnO nanostructures. *Sens. Actuat. B Chem.* **156**, 875–880 (2011).
- Zhang, W. et al. Dynamic and reversible fluorescence imaging of superoxide anion fluctuations in live cells and in vivo. *J. Am. Chem. Soc.* **135**, 14956–14959 (2013).
- Cieslak, A. M. et al. Ultra long-lived electron-hole separation within water-soluble colloidal ZnO nanocrystals: prospective applications for solar energy production. *Nano Energy* **30**, 187–192 (2016).

## Acknowledgements

This work was supported by the TomKat Charitable Trust.

## Author contributions

J.A.R. and S.J.K. conceived, designed and performed the experiments and co-wrote the paper. J.S. assisted with data analysis and paper writing. All authors discussed the results and commented on the manuscript.

## Additional information

**Supplementary information** accompanies this paper at <https://doi.org/10.1038/s42004-019-0153-0>.

**Competing interests:** The authors declare no competing interests.

**Reprints and permission** information is available online at <http://npg.nature.com/reprintsandpermissions/>

**Publisher's note:** Springer Nature remains neutral with regard to jurisdictional claims in published maps and institutional affiliations.



**Open Access** This article is licensed under a Creative Commons Attribution 4.0 International License, which permits use, sharing, adaptation, distribution and reproduction in any medium or format, as long as you give appropriate credit to the original author(s) and the source, provide a link to the Creative Commons license, and indicate if changes were made. The images or other third party material in this article are included in the article's Creative Commons license, unless indicated otherwise in a credit line to the material. If material is not included in the article's Creative Commons license and your intended use is not permitted by statutory regulation or exceeds the permitted use, you will need to obtain permission directly from the copyright holder. To view a copy of this license, visit <http://creativecommons.org/licenses/by/4.0/>.

© The Author(s) 2019